MOLECULAR PLANT PATHOLOGY (2012) 13(2), 160–173 DOI: 10.1111/J.1364-3703.2011.00738.X

Genetic characterization of the HrpL regulon of the fire blight pathogen *Erwinia amylovora* reveals novel virulence factors

R. RYAN MCNALLY[1], IAN K. TOTH[2], PETER J. A. COCK[2], LEIGHTON PRITCHARD[2], PETE E. HEDLEY[3], JENNY A. MORRIS[3], YOUFU ZHAO[4] AND GEORGE W. SUNDIN[1,5,*]

[1]*Department of Plant Pathology, Michigan State University, East Lansing, MI 48824, USA*
[2]*Plant Pathology Programme, The James Hutton Institute, Invergowrie, Dundee DD2 5DA, UK*
[3]*Genetics Programme, The James Hutton Institute, Invergowrie, Dundee DD2 5DA, UK*
[4]*Department of Crop Sciences, University of Illinois, Urbana, IL 61801, USA*
[5]*Center for Microbial Pathogenesis, Michigan State University, East Lansing, MI 48824, USA*

SUMMARY

The bacterial pathogen *Erwinia amylovora* is the causal agent of fire blight, an economically significant disease of apple and pear. Disease initiation by *E. amylovora* requires the translocation of effector proteins into host cells via the hypersensitive response and pathogenicity (*hrp*) type III secretion system (T3SS). The alternative sigma factor HrpL positively regulates the transcription of structural and translocated components of the T3SS via *hrp* promoter elements. To characterize genome-wide HrpL-dependent gene expression in *E. amylovora* Ea1189, wild-type and Ea1189Δ*hrpL* strains were cultured in *hrp*-inducing minimal medium, and total RNA was compared using a custom microarray designed to represent the annotated genes of *E. amylovora* ATCC 49946. The results revealed 24 genes differentially regulated in Ea1189Δ*hrpL* relative to Ea1189 with fold-change expression ratios greater than 1.5; of these, 19 genes exhibited decreased transcript abundance and five genes showed increased transcript abundance relative to Ea1189. To expand our understanding of the HrpL regulon and to elucidate direct versus indirect HrpL-mediated effects on gene expression, the genome of *E. amylovora* ATCC 49946 was examined *in silico* using a hidden Markov model assembled from known *Erwinia* spp. *hrp* promoters. This technique identified 15 putative type III novel *hrp* promoters, seven of which were validated with quantitative polymerase chain reaction based on expression analyses. It was found that HrpL-regulated genes encode all known components of the *hrp* T3SS, as well as five putative type III effectors. Eight genes displayed apparent indirect HrpL regulation, suggesting that the HrpL regulon is connected to downstream signalling networks. The construction of deletion mutants of three novel HrpL-regulated genes resulted in the identification of additional virulence factors as well as mutants displaying abnormal motility and biofilm phenotypes.

*Correspondence: Email: sundin@msu.edu

INTRODUCTION

The enterobacterium *Erwinia amylovora* is the causal agent of fire blight, a devastating disease affecting apple, pear and other rosaceous plants. *Erwinia amylovora* pathogenesis is dependent on the production of a functional type III secretion system (T3SS), the type III effector DspA/E and the exopolysaccharide amylovoran (Oh and Beer, 2005). A T3SS is utilized by Gram-negative bacterial plant pathogens and functions in the delivery of pathogen-derived effector proteins into the host cytoplasm (Büttner and He, 2009). Type III effectors translocated into host cells function to suppress host defences and promote infection (Hogenhout *et al*., 2009). Translocation of the *E. amylovora* type III effector DspA/E is required for pathogenesis and exemplifies the role of the T3SS in the development of fire blight (Barny *et al*., 1990; Bauer and Beer, 1991; Bocsanczy *et al*., 2008; Triplett *et al*., 2009).

Structural, secreted and translocated components of the T3SS are encoded by hypersensitive response and pathogenicity (*hrp*) genes located within a pathogenicity island (PAI) in the *E. amylovora* genome (Barny *et al*., 1990; Bauer and Beer, 1991; Zhao *et al*., 2009a). Other genes encoding type III effectors, such as $avrRpt2_{Ea}$, are located elsewhere in the genome (Zhao *et al*., 2006). In plant pathogens, such as *E. amylovora* and *Pseudomonas syringae*, the ECF-family alternative sigma factor HrpL coordinates the transcription of T3SS genes (Chatterjee *et al*., 2002a; Innes *et al*., 1993; Shen and Keen, 1993; Wei and Beer, 1995).

The regulatory signals culminating in *hrpL* activation begin with environmental stimuli, including unknown plant factors. A specific minimal medium (*hrp*-inducing minimal medium, hrpMM) is used *in vitro* to mimic conditions of the plant apoplast (Wei *et al*., 1992). Although *hrp*-inducing stimuli may or may not be communicated via the two-component signal transduction system *hrpXY* (Wei *et al*., 2000; Zhao *et al*., 2009b), the NtrC-family σ^{54} enhancer protein HrpS is a pathogenicity factor in many T3SS-dependent phytobacteria and is required for *hrpL* transcription in *E. amylovora* and other plant pathogens, including *P. syringae* and other enteric plant pathogens in the genera *Dickeya*, *Pantoea* and *Pectobacterium* (Chatterjee *et al*., 2002b; Hutcheson *et al*., 2001;

Merighi *et al*., 2003; Wei *et al*., 2000; Xiao *et al*., 1994; Yap *et al*., 2005). In addition to *hrpS*, σ^{54} and integration host factor (IHF) are also required for *hrpL* transcription in *Pectobacterium carotovorum* ssp. *carotovorum* Ecc71 (Chatterjee *et al*., 2002b).

The *hrp* promoter is a *cis*-element required for HrpL-mediated transcriptional activity (Innes *et al*., 1993; Shen and Keen, 1993; Wei and Beer, 1995; Xiao and Hutcheson, 1994). In *Pantoea agglomerans* pv. *gypsophilae* 824-1 and *Dickeya dadantii* 3937, HrpL exhibits RNA polymerase-dependent binding to the *hrp* promoter (Nissan *et al*., 2005; Yang *et al*., 2010). Although functional *hrp* promoters exhibit sequence variability (Nissan *et al*., 2005; Vencato *et al*., 2006), conserved motifs allow for the accurate prediction of genes subject to positive HrpL regulation (Ferreira *et al*., 2006; Fouts *et al*., 2002; Vencato *et al*., 2006; Yang *et al*., 2010; Zwiesler-Vollick *et al*., 2002).

Among HrpL-regulated genes, virulence factors not directly related to type III secretion have also been implicated as constituents of the HrpL regulon, most notably the *P. syringae* pv. *tomato* DC3000 phytotoxins syringomycin and coronatine (Fouts *et al*., 2002; Sreedharan *et al*., 2006). In *E. amylovora*, the *hrp* PAI encodes putative phaseolotoxin-like biosynthetic proteins required for systemic fire blight development (Oh *et al*., 2005). Additional virulence roles for HrpL are also suggested by type III secretion-independent *hrpL* mutant phenotypes, including increased peroxidase activity and hypermotility (Cesbron *et al*., 2006; Faize *et al*., 2006).

Global analyses of gene regulation in bacteria have been greatly facilitated by the availability of microarrays. To date, genome-wide microarray analyses of the HrpL regulon have been conducted in *P. syringae* pv. *tomato* DC3000 and *D. dadantii* 3937 (Ferreira *et al*., 2006; Lan *et al*., 2006; Yang *et al*., 2010). In this study, we designed and validated an *E. amylovora* ATCC 49946 microarray and, combined with bioinformatic *hrp* promoter modelling, sought to characterize HrpL-mediated gene expression across the genome of *E. amylovora* Ea1189. Relevant to this study, we hypothesized that: (i) microarray data comparing the gene expression of wild-type (WT) *E. amylovora* with its corresponding *hrpL* mutant would reveal the differential transcription of T3SS genes in *hrp*-inducing medium; (ii) this microarray experiment would identify novel components of the HrpL regulon broader than T3SS genes; and (iii) novel HrpL-regulated genes would play a quantifiable role in fire blight pathogenesis by *E. amylovora*.

RESULTS

HrpL in *E. amylovora* Ea1189 is a pathogenicity factor

In conformity with previous reports in *E. amylovora* Ea321 (Wei and Beer, 1995), the *hrpL* chromosomal deletion mutant Ea1189Δ*hrpL* was nonpathogenic when inoculated into immature pear fruit (Fig. 1). Percentage necrosis measurements at 4 and 6 days post-inoculation (dpi) revealed a complete inhibition of disease development and exemplified the role of *hrpL* as a pathogenicity factor during host infection (Fig. 1). The *hrpL* mutant strain was successfully complemented *in trans* with pRRM1, a clone of *hrpL*, restoring full virulence in the Ea1189Δ*hrpL* mutant (Fig. 1).

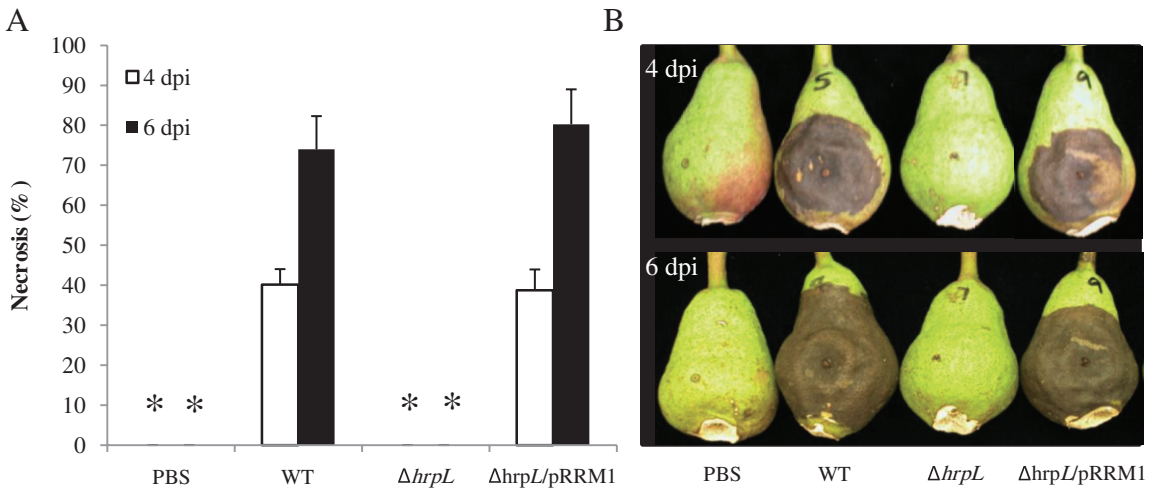

Fig. 1 Immature pear fruit virulence assay. Pear fruits were inoculated with wild-type (WT) Ea1189, Ea1189Δ*hrpL* and Ea1189Δ*hrpL*/pRRM1 complemented *in trans* with full-length *hrpL*. The percentage necrosis was observed and recorded 4 and 6 days post-inoculation (dpi). WT Ea1189 represents a full-virulence positive control. Phosphate-buffered saline (PBS) was used as a negative control. In quantitative measurements of the percentage necrosis (A) and in qualitative imagery of inoculated pears (B), the Ea1189Δ*hrpL* deletion mutant was nonpathogenic at 4 and 6 dpi. Complementation with plasmid-borne *hrpL* (pRRM1) fully restored pathogenicity to Ea1189Δ*hrpL* at all time points measured. *Results significantly different ($P < 0.05$) from WT at same dpi. Error bars represent standard error.

Microarray analyses reveal differential gene expression in Ea1189 and Ea1189Δ*hrpL*

Microarrays represent a genomics tool useful for the rapid identification of differentially regulated genes. To begin the characterization of the HrpL regulon, we developed an oligonucleotide microarray encompassing the annotated genes of the fire blight pathogen *E. amylovora* ATCC 49946. As the two sequenced *E. amylovora* genomes exhibit more than 99.99% sequence conservation (Smits *et al*., 2010) and Agilent arrays utilize long 60-mer oligonucleotide probes, we surmised that this microarray would be applicable to working with any *E. amylovora* strain. On the basis of preliminary quantitative real-time polymerase chain reaction (qRT-PCR) to explore HrpL-mediated gene expression, strains were induced in hrpMM for 6 and 18 h, and total RNA was isolated from WT Ea1189 and Ea1189Δ*hrpL* and subjected to microarray analysis. The results indicated differential gene expression in Ea1189Δ*hrpL* relative to WT Ea1189. In total, 24 genes were found to be differentially regulated with fold-change expression ratios greater than 1.5 (Fig. 2). Of these, 19 genes exhibited direct or indirect positive regulation by HrpL and five genes were negatively regulated. The majority of genes exhibiting HrpL-mediated regulation were identified from RNA extracted at 6 h post-inoculation (hpi) in hrpMM. At 18 hpi, only five genes showed differential expression between WT Ea1189 and Ea1189Δ*hrpL* (Table 1). No gene identified in our microarray analysis displayed HrpL-dependent transcript accumulation at both 6 and 18 hpi, suggesting that the characteristics of the HrpL regulon change dramatically over time (Table 1). No differential expression was observed from the microarray probes for plasmid-encoded genes.

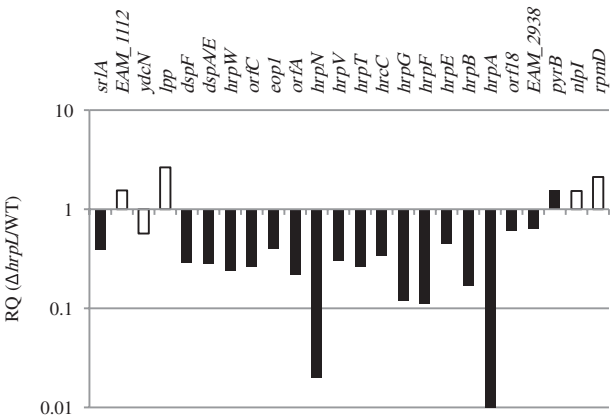

Fig. 2 Microarray expression profile of *in vitro* HrpL regulon comparing RNA extractions from wild-type (WT) Ea1189 and Ea1189Δ*hrpL* after inoculation in hypersensitive response and pathogenicity (*hrp*)-inducing minimal medium (hrpMM) for 6 h (black bars) and 18 h (white bars). Transcript abundance was increased for 19 genes and decreased for five genes in the presence of *hrpL*. Relative quantification (RQ) values satisfied $P < 0.05$ and an expression ratio cut-off of >1.5×.

Positive regulation by HrpL in microarray analysis

The majority of genes displaying HrpL-mediated regulation in hrpMM at 6 hpi encode components of the T3SS, including structural components of the T3SS, such as *hrcC*, the harpins *hrpN* and *hrpW*, effectors *dspA/E* and *eop1*, and type III chaperones *dspF* and *orf*C. Of all genes under HrpL regulation, the pilus subunit gene *hrpA* exhibited the greatest fold change in transcript abundance in Ea1189Δ*hrpL* relative to WT Ea1189 (Table 1). This is compatible with the large number of HrpA subunits presumably required for functional T3SS pilus formation (He and Jin, 2003).

Although T3SS components are transcribed from known *hrp* promoters (Wei and Beer, 1995), our microarray data revealed four individual genes (*srlA*, *orf18*, *EAM_2938* and *ydcN*) at different genomic locations that were up-regulated by HrpL and all lacked recognizable *hrp* promoters (Table 1). *srlA*, *orf18* and *EAM_2938* transcription was dependent on HrpL in hrpMM at 6 hpi (Table 1). The sorbitol permease *srlA* is a known virulence factor utilized during apple shoot infection (Aldridge *et al*., 1997). *orf18* is predicted to encode a VirK-like protein with signal peptides that, although located within the T3SS PAI of *E. amylovora*, remains uncharacterized and lacks a canonical *hrp* promoter upstream of the translational start site (Oh *et al*., 2005). *EAM_2938* encodes an uncharacterized membrane protein. The only gene identified as being positively regulated by HrpL in hrpMM at 18 hpi is *ydcN*, a XRE family transcriptional regulator predicted via sequence similarity to be an uncharacterized *Pantoea* sp. At-9b protein Pat9b_1215 (accession NC_014837.1; E-value 3e-38) using National Center for Biotechnology Information (NCBI) protein–protein BLAST (Table 1). *ydcN* also lacks an *hrp* promoter and, collectively, these results suggest that indirect HrpL regulation takes place, and that the HrpL regulon of *E. amylovora* is part of a larger signalling network interconnected to broader gene regulatory networks.

Negative regulation by HrpL in microarray analysis

Although functionally implicated as a positive regulator of genes important for pathogenesis and hypersensitive response (HR) elicitation, genome-wide analyses of the HrpL regulon in other bacterial plant pathogens have also identified negative HrpL-mediated gene expression (Ferreira *et al*., 2006; Lan *et al*., 2006; Yang *et al*., 2010). Of the 24 genes identified in our microarray study as components of the HrpL regulon, five demonstrated negative regulation by HrpL, i.e. showed an increased transcript abundance in Ea1189Δ*hrpL* (Table 1). The majority of these genes were differentially expressed in hrpMM at 18 hpi, indicating that positive HrpL-mediated gene expression is reduced over time *in vitro* (Table 1). Genes negatively regulated by HrpL in hrpMM at 18 hpi include a lipoprotein with tetratricopeptide repeats, designated *nlpI* (Table 1). The only gene

Table 1 Results of *Erwinia amylovora* wild-type (WT)/Δ*hrpL* microarray analysis 6 and 18 h post-inoculation (hpi) in hypersensitive response and pathogenicity (*hrp*)-inducing minimal medium (hrpMM).

Accession	Gene	Fold change (WT/Δ*hrpL*)	Description	qRT-PCR RQ	Et1/99 orthologue
6 hpi					
EAM_2887	*hrpA**	100	T3SS pilus	0.58 ± 0.1	+
EAM_2877	*hrpN**	40.0	T3SS translocator	0.74 ± 0.1	+
EAM_2882	*hrpF**	9.43	T3SS protein		+
EAM_2881	*hrpG*†	8.55	T3SS protein		+
EAM_2886	*hrpB*†	5.81	T3SS protein		+
EAM_2876	*orfA*†	4.50	T3SS chaperone		+
EAM_2873	*hrpW**	4.20	T3SS translocator		+
EAM_2879	*hrpT*†	3.82	T3SS protein		+
EAM_2874	*orfC*†	3.77	T3SS chaperone		+
EAM_2872	*dspA/E**	3.55	T3SS effector	1.01 ± 0.2	+
EAM_2871	*dspF*†	3.40	T3SS chaperone		+
EAM_2878	*hrpV*†	3.32	T3SS protein		+
EAM_2880	*hrcC*†	2.96	T3SS protein		+
EAM_0521	*srlA*	2.56	Sorbitol permease		–
EAM_2875	*eop1*†	2.48	T3SS effector		+
EAM_2883	*hrpE*†	2.22	T3SS protein		+
EAM_2912	*orf18*	1.63	Hypothetical protein	0.71 ± 0.2	–
EAM_2938	*EAM_2938*	1.57	Membrane protein	0.66 ± 0.1	–
EAM_3054	*pyrB*	–1.54	Carbamoyltransferase	0.71 ± 0.1	+
18 hpi					
EAM_1248	*ydcN*	1.76	XRE transcriptional regulator	1.77 ± 0.1	+
EAM_3066	*nlpI*	–1.53	Tetratricopeptide lipoprotein	2.73 ± 0.1	+
EAM_1112	*EAM_1112*	–1.55	Hypothetical protein	1.56 ± 0.0	–
EAM_3180	*rpmD*	–2.11	50S ribosomal protein L30		+
EAM_1656	*lpp*	–2.64	Membrane lipoprotein	1.40 ± 0.0	+

qRT-PCR, quantitative real-time polymerase chain reaction; RQ, relative quantification; T3SS, type III secretion system; +/–, presence/absence of predicted *E. amylovora* orthologue in *Erwinia tasmaniensis* Et1/99 (Kube *et al*., 2008) with E-value less than 1.00E-04 in National Center for Biotechnology Information (NCBI) protein database. Gene annotations are in accordance with *E. amylovora* ATCC 49946 genome (Sebaihia *et al*., 2010).
*HrpL regulated; has known *hrp* promoter 5′ adjacent to open reading frame.
†Gene is constituent of HrpL-regulated operon in T3SS pathogenicity island (PAI).

negatively regulated by HrpL in hrpMM at 6 hpi is the aspartate carbamoyltransferase catalytic subunit *pyrB* (Table 1).

Identification of *hrp* promoters in *E. amylovora* using hidden Markov modelling

To complement our microarray results, we continued to characterize the HrpL regulon by analysing the occurrence and distribution of *hrp* promoters based on an alignment of 99 known promoter regions from *Erwinia* and *Pseudomonas* species using T-Coffee multiple alignment software (Notredame *et al*., 2000). The consensus motif of this alignment (GGAAC-N18/N19-ACNNA) (Fig. 3A) is less conserved than recent *hrp* promoter alignments reported in *P. syringae* alone (Ferreira *et al*., 2006; Fouts *et al*., 2002). Although comparisons of *hrp* promoter sequence alignments across genera did not reveal stark differences between promoter elements, the –10 motif of *P. syringae hrp* promoters exhibited additional conserved residues (Fig. 3). Therefore, to identify novel *hrp* promoters in *E. amylovora*, a hidden Markov model (HMM) was created from a multiple sequence alignment of 54 *Erwinia*, *Pectobacterium*, *Pantoea* and *Dickeya hrp* promoters (Fig. 3C) and tested against the genome of *E. amylovora* ATCC 49946 using HMMer 2.3.2 biosequence analysis software (Eddy, 1998). Thirty *hrp* promoters were predicted with a bit-score classifier threshold of 8.5 (Table 2). Eleven of the predicted *hrp* promoters are positioned upstream of open reading frames or operons encoding T3SS components including all known structural, secreted and translocated T3SS proteins. Of a further 19 putative *hrp* promoters, *hsvA*, *orf12* and *orf19* are located on the T3SS PAI, although their respective contributions to type III secretion and translocation are unknown (Oh *et al*., 2005).

The remaining candidate *hrp* promoters are not oriented to transcribe mRNA related to type III secretion (Table 2) and may be involved in the regulation of the expression of other virulence factors, consistent with observations in *E. amylovora* that *hrpL* mutants exhibit increased peroxidase activity relative to type III secretion null strains and that *hrpL* mutants are also hyperflagellated and more motile than WT *E. amylovora* (Cesbron *et al*., 2006; Faize *et al*., 2006).

Verification of microarray and HMMer data with qRT-PCR

To validate *hrpL* gene expression patterns observed in our microarray analysis and to verify the HrpL-dependent activity of novel

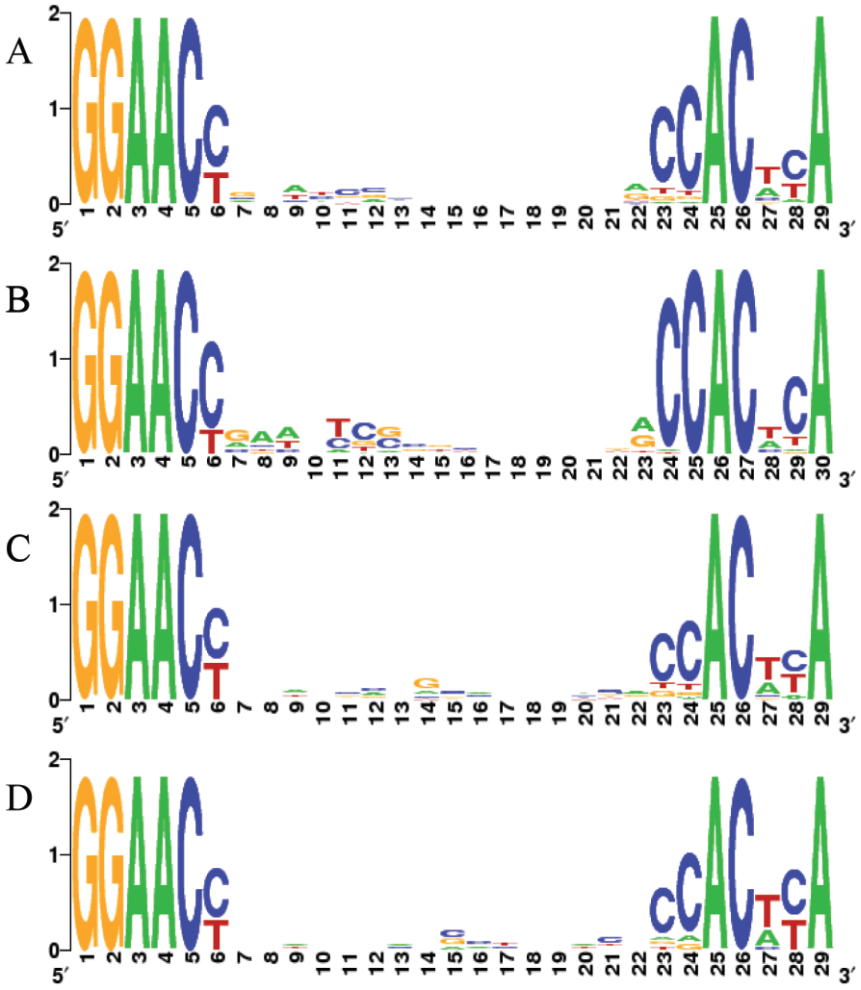

Fig. 3 T-Coffee multiple sequence alignment of hypersensitive response and pathogenicity (*hrp*) promoters. Weblogo was used to visualize the alignments of 99 *hrp* promoters from phytopathogenic pseudomonads and *Erwinia* species (A), 45 *hrp* promoters collected from *Pseudomonas syringae* pathovars (B), 54 *hrp* promoters collected from *Erwinia*, *Pectobacterium*, *Dickeya* and *Pantoea* spp. (C) and 13 *hrp* promoters from *Erwinia amylovora* (D). *hrp* promoter motifs are broadly conserved across phytopathogenic bacteria excluding additionally conserved cytosine residues 5′ of the −10 motif in *Pseudomonas* spp.

hrp promoters predicted using HMM 2.3.2, 20 genes based on results from the microarray and HMMer analyses were selected for expression profiling. RNA was extracted from WT Ea1189 and Ea1189Δ*hrpL* after induction in hrpMM for 6 and 18 h and subjected to qRT-PCR analysis. qRT-PCR expression results in triplicate confirm HrpL-mediated transcript accumulation for 18 genes (Table 2). These results are in agreement with our microarray data and highlight eight novel *hrp* promoters predicted via hidden Markov modelling. On the basis of 22 hrp promoters experimentally verified with microarray expression data and qRT-PCR, the conserved *hrp* promoter in *E. amylovora* is 5′-GGAAC-$N_{(16–20)}$-ACNNC-3′ and averages 88 nucleotides 5′ adjacent of an HrpL-regulated gene (Table 2). These characteristics are largely consistent with previously reported *hrp* promoter motifs with the exception of the conjugative transfer gene *traF* and a predicted exported lipoprotein *yfiM*, both of which exhibit −35 and −10 promoter motifs separated by an abnormal number of nucleotides, 16 and 20, respectively (Table 2).

Mutational analyses of HrpL-regulated genes

Although HrpL is required for the transcriptional promotion of the T3SS (Chatterjee *et al*., 2002a; Innes *et al*., 1993; Shen and Keen, 1993; Wei and Beer, 1995), the HrpL regulon is also implicated in additional regulatory activities such as motility (Cesbron *et al*., 2006; Ortiz-Martin *et al*., 2010). To determine the biological relevance of genes regulated by HrpL, several chromosomal mutations were generated in Ea1189. These mutants were assayed for phenotypes related to factors important for fire blight pathogenesis, including virulence, biofilm formation and swarming motility. Ea1189Δ*EAM_2938*, Ea1189Δ*ydcN* and Ea1189Δ*nlpI* were all significantly less virulent than WT Ea1189 in immature pear assays measured at 4 and 6 dpi (Fig. 4A,B). *EAM_2938*, *ydcN* and *nlpI* have not been shown previously to contribute to the virulence of *E. amylovora*. *orf18*, an HrpL-regulated constituent of the T3SS PAI in *E. amylovora*, appeared not to play a quantifiable role in virulence (Fig. 4B). The *ydcN* mutant strain was complemented with pRRM2, a clone of *ydcN*, restoring virulence in the Ea1189Δ*ydcN*

Table 2 Results of hypersensitive response and pathogenicity (*hrp*) promoter modelling and quantitative real-time polymerase chain reaction (qRT-PCR) analysis.

Annotation	Gene	HMM (E-value)	Description	qRT-PCR RQ	Et1/99	Position (nt from ORF)	nt b/t motifs
Type III secretion							
EAM_2780	*eop2*	6.0E-05	T3SS helper	0.60 ± 0.1	–	–139	18
EAM_2887	*hrpA**	2.5E-04	T3SS pilus	0.58 ± 0.1	+	–058	18
EAM_2882	*hrpF**	4.9E-04	T3SS protein		+	–033	19
EAM_2895	*hrpJ*	9.7E-04	T3SS protein	0.57 ± 0.1	+	–035	18
EAM_2873	*hrpW**	1.2E-03	T3SS translocator		+	–059	18
EAM_2877	*hrpN**	1.2E-03	T3SS translocator	0.74 ± 0.1	+	–077	18
EAM_2911	*hrpK*	1.5E-03	T3SS protein	0.57 ± 0.1	–	–036	18
EAM_2697	$hopC_{Ea}$	1.8E-03	T3SS effector	0.57 ± 0.1	–	–031	18
EAM_0423	$avrRpt2_{Ea}$	2.8E-03	T3SS effector	0.61 ± 0.1	–	–032	18
EAM_2872	*dspA/E**	4.6E-03	T3SS effector	1.01 ± 0.2	+	–042	18
EAM_2190	*eop3*	6.5E-03	T3SS effector	0.54 ± 0.1	–	–551	19
Other							
EAM_2611	*yfiM*	5.0E-04	Exported lipoprotein	0.50 ± 0.1	+	–173	16
EAM_2913	*orf19*	7.2E-04	Lysozyme inhibitor	0.40 ± 0.0	+	–076	18
EAM_1557	*invG*	8.3E-04	Non-*hrp* T3SS protein		+	–122	20
EAM_2938	*EAM_2938**	8.9E-04	Membrane protein	0.66 ± 0.1	–	–126	18
EAM_0268	*traF*	1.2E-03	Conjugation protein	0.53 ± 0.1	+	–156	20
EAM_1012	*EAM_1012*	1.3E-03	Hypothetical protein	0.64 ± 0.1	–	–043	18
EAM_1472	*ybhH*	1.3E-03	Hypothetical protein	0.58 ± 0.1	–	–211	18
EAM_2695	*cysJ*	1.6E-03	Sulphite reductase		+	–013	16
EAM_2906	*orf12*	1.7E-03	*N*-Acyltransferase	0.50 ± 0.1	+	–031	18
EAM_2195	*aroQ*	2.2E-03	Chorismate mutase	0.48 ± 0.1	–	–083	19
EAM_2951	*fimD*	3.2E-03	Fimbrial usher	0.96 ± 0.2	+	–034	17
EAM_2910	*hsvA*	3.4E-03	Amidinotransferase	0.38 ± 0.1	–	–098	18
EAM_3434	*ompA*	4.4E-03	Membrane protein		+	–079	22
EAM_1462	*yceG*	4.8E-03	Chorismate lyase		+	–014	15
EAM_2175	*terC*	5.1E-03	Membrane protein		+	–678	16
EAM_0252	*yjbB*	5.9E-03	Symporter		+	–114	16
EAM_2456	*yaiL*	6.2E-03	Hypothetical protein		+	–115	16
EAM_2572	*fliN*	6.3E-03	Flagellar motor switch	0.55 ± 0.1	+	–199	18
EAM_0855	*yafS*	6.5E-03	Methyltransferase		+	–283	24

HMM, hidden Markov model; nt, nucleotide; nt b/t motifs, number of nucleotides between the –35 and –10 promoter regions; ORF, open reading frame; RQ, relative quantification; +/–, presence/absence of predicted *Erwinia amylovora* orthologue in *Erwinia tasmaniensis* Et1/99 with E-value less than 1.00E-04 in National Center for Biotechnology Information (NCBI) protein database.

*Identified as HrpL regulated in wild-type (WT)/Δ*hrpL* microarray analysis.

mutant. The addition of pRRM3 to Ea1189Δ*EAM_2938* and pRRM4 to Ea1189Δ*nlpI* did not result in the complementation of the cognate mutant phenotypes, probably as a result of pleiotropic effects.

Although known to play a role in the regulation of the T3SS (Chatterjee *et al*., 2002a; Innes *et al*., 1993; Shen and Keen, 1993; Wei and Beer, 1995), previous examinations of HrpL function have also demonstrated that the HrpL regulon includes genes whose activity is not directly related to type III secretion (Cesbron *et al*., 2006; Faize *et al*., 2006; Sreedharan *et al*., 2006; Yap *et al*., 2005). To better understand the diversity of phenotypes observed in Δ*hrpL* strains, mutants in our selected HrpL-regulated genes were assayed for alterations in their biofilm formation and motility phenotypes. To examine swarming motility, mutants of Ea1189Δ*EAM_2938*, Ea1189Δ*orf18*, Ea1189Δ*ydcN* and Ea1189Δ*nlpI* were measured at 2 and 4 dpi. To assay biofilm formation, these mutants were also cultured in the presence of glass cover-slips for 48 h and stained with crystal violet prior to spectrophotometric analysis. In both assays, Ea1189Δ*ydcN* and Ea1189Δ*nlpI* demonstrated increased biofilm formation and decreased swarming motility relative to WT Ea1189 (Fig. 4C,D).

Analysis of the *EAM_2938* gene

In response to observations that *EAM_2938* is positively regulated by HrpL (Fig. 2; Table 1), contains a novel *hrp* promoter (Table 2) and that the mutant Ea1189Δ*EAM_2938* exhibits a strong loss-of-virulence phenotype (Fig. 4A,B), the *EAM_2938* gene was subjected to bioinformatic analyses. Using the operon finding package FGENESB (Tyson *et al*., 2004), *EAM_2938* is predicted to be the first open reading frame in an operon upstream of *EAM_2937*, *EAM_2936* and *EAM_2935* (Fig. 5). To determine whether *hrpL* can direct the transcriptional activation of genes downstream of *EAM_2938*, qRT-PCR was conducted to study the expression of genes downstream of *EAM_2938* using RNA extractions from WT Ea1189 and Ea1189Δ*hrpL* after induction in hrpMM for 6 h. The

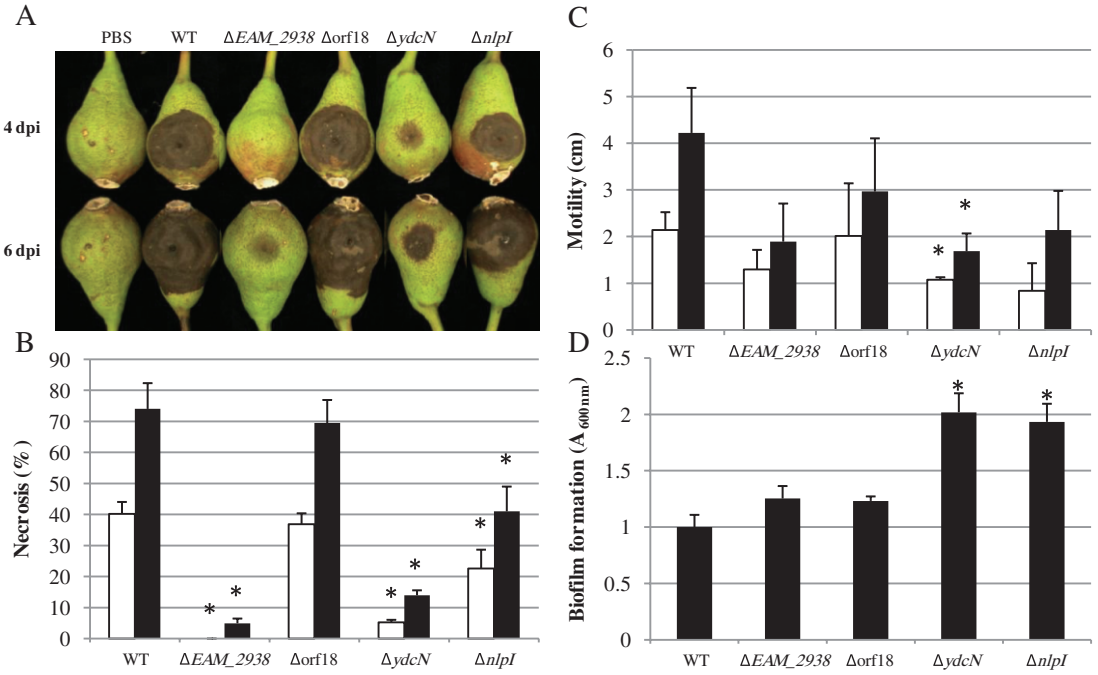

Fig. 4 Phenotypic characterization of HrpL-regulated mutant strains in Ea1189. Four genes, *EAM_2938*, *orf18*, *ydcN* and *nlpI*, were deleted from the chromosome of Ea1189 via λ red recombinase. Symptoms of Ea1189Δ*EAM_2938*, Ea1189Δ*orf18*, Ea1189Δ*ydcN* and Ea1189Δ*nlpI* in immature pear fruit at 4 and 6 days post-inoculation (dpi) (A) (PBS, phosphate-buffered saline) and percentage area of necrosis in immature pear fruit at 4 dpi (white) and 6 dpi (black) (B). Quantification of cellular motility at 2 dpi (white) and 4 dpi (black) (C) and biofilm formation (D) of Ea1189Δ*EAM_2938*, Ea1189Δ*orf18*, Ea1189Δ*ydcN* and Ea1189Δ*nlpI*. *Results were significantly different from wild-type (WT) Ea1189 at the same time point at $P < 0.05$. Error bars represent standard error.

	2938	2937	2936	2935
%GC	42	45	49	54
RQ	0.66±0.07	0.59± 0.07	0.56±0.06	0.57±0.06
E-value	4e-07/ XBJ1_3905•	9e-45/ XNC1_3917#	7e-63/ SVI_1964°	0.0/ PC1_0062▪

Fig. 5 *EAM_2938* gene cluster including GC content (% GC) of individual genes relative to *Erwinia amylovora* (53.6%), quantitative real-time polymerase chain reaction (qRT-PCR) relative quantification (RQ) of wild-type (WT)/Δ*hrpL* transcript abundance, and E-values and homologues determined using National Center for Biotechnology Information (NCBI) protein BLAST analysis. *Exhibits putative transmembrane domains predicted using Dense Alignment Surface (DAS) method software. ‡Displays signal peptide, predicted using SignalP 3.0. ●, Homologue found in *Xenorhabdus bovienii* SS-2004 (accession NC_013892); #, homologue found in *Xenorhabdus nematophila* ATCC 19061 (accession NC_ 014228); ○, homologue found in *Shewanella violacea* DSS12 (accession NC_ 014012); ■, homologue found in *Pectobacterium carotovorum* PC1 (accession NC_ 012917).

results indicate that *EAM_2938*, *EAM_2937*, *EAM_2936* and *EAM_2935* are all differentially regulated by HrpL, suggesting that *EAM_2938* may be the first gene in an HrpL-regulated operon (Fig. 5). On the basis of protein–protein NCBI database searches, *EAM_2937* encodes a disulphide bond-forming inner membrane protein, *EAM_2936* encodes a phytochelatin synthase-like protein and the EAM_2935 protein is a predicted γ-glutamyltranspeptidase (Fig. 5). The EAM_2938 and EAM_2937 proteins are expected to be membrane localized with putative transmembrane regions predicted via the Dense Alignment Surface (DAS) analytical server (Fig. 5). SignalP 3.0 indicates that the phytochelatin synthase-like gene, *EAM_2936*, encodes a putative exported protein as a result of the presence of a signal peptide (Fig. 5).

EAM_2938 represents a novel virulence factor in Ea1189. To determine the distribution of EAM_2938 orthologues among phytopathogenic bacteria, the NCBI protein database was searched for amino acid sequences with significant sequence conservation. Interestingly, the presence of *EAM_2938* appears to be unique to *E. amylovora* relative to other bacterial plant pathogens (Fig. 5). Similarly, the downstream genes *EAM_2937* and *EAM_2936* are also not broadly conserved in known plant pathogens, excluding

the closely related species *E. pyrifoliae* (Fig. 5). In addition, GC-profile software calculated that *EAM_2938* exhibits 42% GC content (Fig. 5). The average GC content of the sequenced genome of *E. amylovora* is 53.6% (Sebaihia *et al*., 2010; Smits *et al*., 2010), suggesting that *EAM_2938* (42%), as well as *EAM_2937* (45%) and *EAM_2936* (49%), may have been recently acquired by the *E. amylovora* genome.

DISCUSSION

In this study, we explored the HrpL regulon of the fire blight pathogen *E. amylovora* using a combination of techniques, including microarray, bioinformatics and qRT-PCR, and identified 39 genes that exhibited HrpL-dependent transcriptional activity. Mutational analyses of the constituents of the HrpL regulon revealed novel virulence factors with differential biofilm formation and motility phenotypes. Our results suggest that the HrpL regulon is interconnected with downstream signalling networks and that HrpL-regulated genes, in addition to those with predicted roles in type III secretion, are important in fire blight pathogenesis.

As in previous analyses of the HrpL regulon in other plant pathogenic bacteria, including *P. syringae* pv. *tomato* DC3000 and *D. dadantii* Ech3937 (Ferreira *et al*., 2006; Fouts *et al*., 2002; Yang *et al*., 2010), the HrpL regulon in *E. amylovora* encompasses genes regulated directly (via the *hrp* promoter) as well as indirectly. Of the 24 genes identified in our microarray, 16 genes were up-regulated directly in the presence of functional *hrpL*. All genes identified in our microarray analysis that appeared to be regulated directly by HrpL, excluding *EAM_2938*, have been characterized or have predicted roles in type III secretion. These results exemplify the role of *hrpL* in coordinating the expression of type III secretion genes and are in accordance with previous genome-wide demonstrations of the role of *hrpL* in type III secretion (Ferreira *et al*., 2006; Fouts *et al*., 2002; Lan *et al*., 2006; Yang *et al*., 2010).

The type III effector repertoire of *P. syringae* pv. *phaseolicola* 1448A has been reported to include 27 candidates (Vencato *et al*., 2006). Our combined results, including *hrp* promoter modelling and qRT-PCR, demonstrate the existence of only five effector-like genes (*eop1*, *eop3*, *avrRpt2*$_{Ea}$, *dspA/E* and *hopPtoC*$_{Ea}$) subject to direct HrpL regulation (Table 2). The translocation of DspA/E is known to be required for the pathogenesis of *E. amylovora*, but the comprehensive role of DspA/E in facilitating disease development remains elusive (Triplett *et al*., 2009). *avrRpt2*$_{Ea}$ exhibits homology to AvrRpt2 in *P. syringae* pv. *tomato* and is a known virulence factor in pear that is capable of eliciting the HR in Arabidopsis RPS2 when heterologously expressed from *P. syringae* pv. *tomato* DC3000 (Zhao *et al*., 2006). Both *dspA/E* and *hopPtoC*$_{Ea}$ are induced in an immature pear fruit *in vivo* expression technology (IVET) screen, but mutations in *hopPtoC*$_{Ea}$ do not result in a quantifiable virulence defect or reduction in colonization in immature pear virulence assays (Zhao *et al*., 2005). Eop1 and Eop3 are YopJ and HopX homologues, respectively, and, together with DspA/E and *AvrRpt2*$_{Ea}$, were identified in mass spectrometric analysis of the T3SS-dependent secretome of *E. amylovora* ATCC 49946 (Nissinen *et al*., 2007). Mutations in *eop1* have no effect on virulence (Asselin *et al*., 2006), and the functional role of *eop3* remains uncharacterized.

Hidden Markov modelling for *in silico* genome-wide identification of conserved *cis*-elements is a tested strategy for predicting genes under direct *hrp* promoter-mediated transcription by HrpL (Ferreira *et al*., 2006; Vencato *et al*., 2006). To find other genes directly up-regulated by HrpL, a hidden Markov model was assembled from an *Erwinia* spp. *hrp* promoter alignment. Using HMMer 2.3.2, our model identified 30 putative *hrp* promoters in the genome of *E. amylovora* ATCC 49946, including all known components of the T3SS. Using qRT-PCR verification of hrpMM-induced WT Ea1189 and Ea1189Δ*hrpL* RNA extracts, 19 *hrp* promoters were verified as regulated by HrpL, seven of which represent novel components of the HrpL regulon of Ea1189 not identified using microarray analysis, presumably as a result of increased qRT-PCR sensitivity towards low-copy-number transcripts.

EAM_2938 represents a novel HrpL-regulated gene first identified as being differentially expressed in our microarray analysis of WT Ea1189 and Ea1189Δ*hrpL*. HrpL-mediated up-regulation of *EAM_2938* was confirmed using qRT-PCR, and promoter modelling identified a candidate *hrp* promoter 126 nucleotides upstream of the translational start site of EAM_2938. Most notably, a chromosomal deletion of *EAM_2938* severely attenuated virulence in immature pear fruit. Three open reading frames downstream of *EAM_2938* were also regulated by HrpL, suggesting that *EAM_2938*, *EAM_2937*, *EAM_2936* and *EAM_2935* may constitute a novel HrpL-regulated operon. *EAM_2938*, *EAM_2937* and *EAM_2936* are not broadly conserved in other bacterial plant pathogens and exhibit a differential GC content, suggesting that the *EAM_2938* gene cluster may be a recently acquired virulence determinant(s) in Ea1189. Understanding the function of this cluster is therefore important for a better understanding of fire blight development by *E. amylovora*. Interestingly, the EAM_2937 protein (GenBank: DX936506) is a putative inner membrane protein that was identified by Wang and Beer (2006) via a signature-tagged mutagenesis screen as a pathogenicity factor in apple shoot infection, providing additional evidence that the HrpL-regulated *EAM_2938* gene cluster is an important component of pathogenesis by *E. amylovora*.

Two additional *hrp* promoters were also identified via bioinformatics and experimentally confirmed using qRT-PCR, including the conjugative transfer protein *traF* and a chorismate mutase *aroQ*. Although both genes remain uncharacterized, mass spectrometric analysis of the *in vitro* secretome of *E. amylovora* previously identified HrpL-dependent *in vitro* secretion of TraF (Nissinen *et al*., 2007). Our data support this observation and collectively suggest that functional *hrp* promoters in *E. amylovora* can exhibit a

noncanonical number of nucleotides between the −35 and −10 conserved *hrp* promoter motifs. In *E. amylovora* and *D. dadantii*, chorismate mutase gene expression was identified using *in vivo* expression techniques (Yang *et al*., 2004; Zhao *et al*., 2005), and a signature-tagged mutagenesis screen identified chorismate mutase as an *E. amylovora* pathogenicity factor required for apple shoot infection (Wang and Beer, 2006). Chorismate mutase is part of the shikimate metabolic pathway and may be required for normal growth and development, but recent analyses have indicated that chorismate mutase may contribute to plant–nematode and plant–bacterium interactions (Degrassi *et al*., 2010; Jones *et al*., 2003).

Promoter modelling is a useful tool for the identification of genes regulated directly by HrpL via its cognate *hrp* promoter. Although *hrp* promoter-driven gene expression is a prerequisite for many plant–bacterium interactions, genome-wide microarray analysis allows for the detection of genes regulated indirectly. The HrpL regulon is known to include genes regulated indirectly as well directly (Ferreira *et al*., 2006; Lan *et al*., 2006; Yang *et al*., 2010). Our microarray analysis uncovered eight genes that appear to be up- and down-regulated indirectly by functional *hrpL*. The XRE family transcriptional regulator *ydcN* exhibited indirect up-regulation in Ea1189 strains. In hrpMM at 18 hpi, *ydcN* was the only gene exhibiting positive HrpL-mediated expression. XRE transcription factors are broadly conserved across bacterial species and bind DNA, generally resulting in the repression of target gene expression (Barragan *et al*., 2005; Gerstmeir *et al*., 2004; Kiely *et al*., 2008). Consequently, YdcN may connect the HrpL regulon to other signalling networks suppressing the transcription of genes at 18 hpi. Phenotypic analysis of Ea1189Δ*ydcN* revealed a strong attenuation of virulence in immature pear, a decrease in motility and hyper-biofilm formation.

In our microarray analysis of the HrpL regulon, five genes appear to be down-regulated indirectly. For the 50S ribosomal protein *rpmD*, this is consistent with Lan *et al*. (2006), who reported that ribosomal proteins represent the largest group of HrpL-down-regulated genes in *P. syringae* pv. DC3000. Aspartate carbamoyltransferase *pyrB* also exhibited HrpL-mediated down-regulation. In a transposon mutagenesis screen for *E. amylovora* virulence factors, Wang and Beer (2006) identified *pyrB* as a pathogenesis factor required for disease activity in glasshouse-grown apple shoots. The down-regulation of a pathogenicity factor by HrpL at 6 hpi suggests that disease development by *E. amylovora* is temporal in nature, requiring specific pathogenicity and virulence factors at different stages of infection. Like *pyrB*, the lipoprotein *nlpI* was also down-regulated by HrpL in hrpMM at 18 hpi. When inoculated into immature pear, Ea1189Δ*nlpI* displayed a quantifiable decrease in virulence. Further phenotypic characterization of the *nlpI* mutant strain found that, like Ea1189Δ*ydcN*, Ea1189Δ*nlpI* exhibits reduced motility and increased biofilm formation. In *Escherichia coli*, *nlpI* is a confirmed outer membrane protein with conserved tetratricopeptide repeats (Teng *et al*., 2010; Wilson *et al*., 2005). In a screen for *Escherichia coli* mutant strains with abnormal extracellular DNA phenotypes, *nlpI* was identified as a negative regulator of extracellular DNA export (Sanchez-Torres *et al*., 2010). Extracellular DNA has been increasingly recognized as an important component of biofilm matrices, and continued analysis of Ea1189Δ*nlpI* may help to understand the role of extracellular DNA in plant pathogenesis. We have determined previously that biofilm formation is critical to *E. amylovora* virulence and to cell migration within apple xylem (Koczan *et al*., 2009). To date, *nlpI* is the first HrpL-down-regulated gene to be implicated in disease development. Of note, the HrpL regulon is suppressed in nutrient-rich medium (Wei *et al*., 1992), and the characterization of HrpL-mediated gene expression in nutrient-rich medium may identify additional genes down-regulated by HrpL involved in adaptation to nutrient-rich host niches, such as flower nectaries; an important infection court for fire blight development. Collectively, *nlpI*, *ydcN* and *EAM_2938* represent novel virulence factors in *E. amylovora*.

Microarray technology enables the simultaneous characterization of an entire transcriptome in response to different environmental stimuli. Twenty-four genes were differentially regulated in response to the presence of *hrpL*, including nine genes unrelated to the T3SS. Hidden Markov modelling and bioinformatics supported our findings and further allowed us to identify 15 novel predicted *hrp* promoters, seven of which were verified as responsive to functional *hrpL* via qRT-PCR. Taken together, these data suggest that the HrpL regulon of *E. amylovora* encompasses more than just T3SS regulation and may communicate directly or indirectly with other signalling networks to coordinate gene expression during pathogenesis.

EXPERIMENTAL PROCEDURES

Bacterial strains and growth conditions

The bacterial strains and plasmids used in this study are listed in Table 3. All bacterial strains used in this study were cultured in Luria–Bertani (LB) broth unless otherwise noted. All strains were grown at 28 °C in a shaking incubator. Where appropriate, media were supplemented with 50 μg/mL ampicillin, 20 μg/mL chloramphenicol or 12 μg/mL oxytetracycline.

Deletion mutagenesis

Nonpolar chromosomal mutants were generated in *E. amylovora* using the phage λ red recombinase system described previously (Datsenko and Wanner, 2000). Briefly, we transformed *E. amylovora* strain Ea1189 with the helper plasmid pKD46 encoding recombinases red β, γ and exo. Ea1189/pKD46 was grown overnight at 28 °C in a shaking incubator, re-inoculated in LB broth supplemented with 0.1% L-arabinose and cultured for 4–6 h to exponential phase [optical density at 600 nm (OD_{600}) = 0.8]. Cells were made electrocompetent and stored at −80 °C.

Table 3 Bacterial strains, plasmids and primers used in this study.

Strains and plasmids	Relevant characteristics*	Source or reference
Escherichia coli strain		
DH5α	F⁻ 80dlacZ ΔM15 Δ(lacZYA-argF)U169 endA1 recA1 hsdR17(r_K–m_K+) deoR thi-1 supE44 gyrA96 relA1 λ-	Invitrogen, Carlsbad, CA, USA
Erwinia amylovora strains		
Ea1189	Wild-type	Burse *et al*., 2004
Ea1189Δ*hrpL*	*hrpL* deletion mutant, Cm^R	This study
Ea1189Δ*EAM_2938*	*EAM_2938* deletion mutant, Cm^R	This study
Ea1189Δ*ydcN*	*ydcN* deletion mutant, Cm^R	This study
Ea1189Δ*nlpI*	*nlpI* deletion mutant, Cm^R	This study
Ea1189Δ*orf18*	*orf18* deletion mutant, Cm^R	This study
Plasmids		
pBBR1-MCS3	Tc^R, broad-host-range cloning vector	Kovach *et al*., 1995
pRRM1	Tc^R, pBRR1-MCS3 containing *hrpL*	This study
pRRM2	Tc^R, pBRR1-MCS3 containing *ydcN*	This study
pRRM3	Tc^R, pBRR1-MCS3 containing *EAM_2938*	This study
pRRM4	Tc^R, pBRR1-MCS3 containing *nlpI*	This study
pKD3	Amp^R, CmR, mutagenesis cassette template	Datsenko and Wanner, 2000
pKD46	Amp^R, expresses λ red recombinase	Datsenko and Wanner, 2000
Primers		
hrpLKO.F	5′-GGAGCAAGCCATGACAGAAATTCACCTGCAAACA ACTGAATCAACATCGGGTGTAGGCTGGAGCTGCTTC-3′	This study
hrpLKO.R	5′-TTAAGAAAATACTGACTGTTTCAGCGTGACGCGC GCACGCGACAGACGTGCATATGAATATCCTCCTTA-3′	This study
EAM_2938KO.F	5′-ATGTATATGTATTTACCCTTTTTACTAGGCGCAGG CATTGTTTTTAGTATGTGTAGGCTGGAGCTGCTTC-3′	This study
EAM_2938KO.R	5′-CTAGAACGAAAGGAGAAGCGCAGTGGTGGCATG AACTTTCAACCACGCGACATATGAATATCCTCCTTA-3′	This study
EAM_orf18KO.F	5′-ATGATCAAAAAAACACTTCTTGCCGCTATGTTCGC GGGTACATGCAGTACGTGTAGGCTGGAGCTGCTTC-3′	This study
EAM_orf18KO.R	5′-TTATGGCGCGGTGTAAAATTGCGCGCCGCTGCCG ATTTTGCAGTTCCAGCCATATGAATATCCTCCTTA-3′	This study
EAM_3066KO.F	5′-ATGAAGCCATTTTTGCGCTGGTGTCTCGTTGCGAC GGCTTTATCGTTGGCGTGTAGGCTGGAGCTGCTTC-3′	This study
EAM_3066KO.R	5′-CTATTGCTGGTCAGATTCTGATAAATCGTCTTGT GTCTGGCCGAGTAGCGCATATGAATATCCTCCTTA-3′	This study
EAM_1248KO.F	5′-TTGCTCAATCGCCTGTGCCACCTCTATGGCTTCA CCCTGTCACGCTTGTTGTGTAGGCTGGAGCTGCTTC-3′	This study
EAM_1248KO.R	5′-TCATGGGCGAGCCACCACCAGCGCATAGTGCGCC CCCGTGGCCTCCGGCGCATATGAATATCCTCCTTA-3′	This study
hrpL(sacI).F	5′-GTGCATGAGCTCAGCAGTTGTCATTGTGTGGTGC-3′	This study
hrpL(kpnI).R	5′-ACTGACGGTACCGTAAACATTGTTTACCTGATTAGGCTG-3′	This study
ydcN(kpnI).F	5′-ATGCTAGAGGTACCCTTGCTCAATCGCCTGTGCCAC-3′	This study
ydcN(sacI).R	5′-TCGATTCGGAGCTCTCATGGGCGAGCCACCACC-3′	This study

*Cm^R, Tc^R and Amp^R indicate resistance to chloramphenicol, oxytetracycline and ampicillin, respectively.

Recombination fragments encoding acetyltransferase cassettes flanked by 50-nucleotide arms homologous to target genes were synthesized using PCR with plasmid pKD3 as template. Recombination fragments were purified and concentrated using a PCR purification kit (Qiagen, Valencia, CA, USA), and electroporated into competent Ea1189. Putative mutants were screened on selective LB agar medium amended with chloramphenicol. Single-gene recombinatorial deletion was confirmed using PCR (Table 3) and functional complementation.

DNA manipulation and cloning

Restriction enzyme digestion, T4 DNA ligation and PCR amplification of genes were conducted using standard molecular techniques (Sambrook *et al*., 1989). DNA extraction, PCR purification, plasmid extraction and isolation of DNA fragments from agarose were performed with related kits (Qiagen). All DNA was sequenced at the Research Technology Support Facility at Michigan State University, East Lansing, MI, USA. To complement mutant strains, primer pairs were designed with restriction sites for double digestion and directional ligation into pBBR1MCS3 (Kovach *et al*., 1995). Final constructs were transformed into competent Ea1189 by electroporation and screened on LB agar plates amended with oxytetracycline.

Virulence assay

The virulence of Ea1189 strains was determined using a standard immature pear fruit assay, as described previously (Zhao *et al*., 2005). In brief, bacterial strains were cultured overnight, washed and resuspended in 0.5 × phosphate-buffered saline (PBS) to 1×10^3–1×10^4 colony-forming units

(cfu)/mL. Immature pear fruits (*Pyrus communis* L. cv. Bartlett) were surface sterilized with 10% bleach, dried in a laminar flow hood and pricked with a needle prior to the application of 2 μL of bacterial suspension. Inoculated pears were incubated at 28 °C in humidified chambers. Symptoms were recorded at 4 and 6 dpi. The experiments were repeated three times with six replications per experiment. Virulence was determined quantitatively via the percentage necrosis, calculated as the surface area of pear relative to the surface area of necrotic and water-soaked tissue.

Microarray design

An oligonucleotide microarray was designed at the James Hutton Institute [JHI; formerly Scottish Crop Research Institute (SCRI)], and synthesized by Agilent Technologies, Inc. (Palo Alto, CA, USA). Each slide contained eight arrays and each array had nearly 15 000 spots, containing our probes in triplicate. The main *E. amylovora* ATCC 49946 genome (accession NC_013971; Sebaihia *et al*., 2010) had 3483 target sequences (annotated genes and pseudogenes), plus a further 483 target genes or simple gene predictions from five sequenced plasmids: plasmids 1 and 2 for the same strain (accessions NC_013972, NC_013973; McGhee and Jones, 2000; Sebaihia *et al*., 2010), pEL60 and pEU30 (accessions NC_005246, NC_005247; Foster *et al*., 2004) and pEI70 (Spanish strain *Erwinia amylovora* IVIA1614-2a, unpublished; M. M. Lopez and P. Llop, personal communication).

Up to five sense orientation candidate probes per target were designed with the Agilent eArray webtool, using temperature matching methodology, a preferred probe melting temperature of 80 °C, no 3′ bias and a target length of 60 bp. Any short probes were later extended to 60 bp using the Agilent linker. BLASTN (Altschul *et al*., 1997) and Biopython (Cock *et al*., 2009) were used to identify potential cross-hybridization in order to rank the candidate probes. The selection of one probe per genome target, and up to five probes per plasmid target, allowed all of our probes to be present in triplicate.

RNA isolation and microarray execution

Ea1189 WT and *hrpL* mutant (Δ*hrpL*) strains were cultured overnight in LB broth at 28 °C in a shaking incubator and collected the following day via centrifugation at 2300 ***g*** in a microcentrifuge. Each strain was washed once in hrpMM (Huynh *et al*., 1989) before resuspension in hrpMM to 0.6 OD_{600}. Strains were then incubated for 6 and 18 h at 180–200 r.p.m. in a shaking incubator at 18 °C. RNA was extracted from 1 mL of the resultant cultures using an SV Total RNA Isolation System (Promega, Madison, WI, USA) as described by the manufacturer. All RNA was quantified using a NanoDrop ND-100 spectrophotometer (NanoDrop Technologies, Wilmington, DE, USA) and quality checked using an RNA 6000 Nano Kit on a 2100 Bioanalyzer (Agilent Technologies). Fluorescent labelling of total RNA was performed as described previously (Venkatesh *et al*., 2006) using the following experimental array design on a single 8 × 15k format slide: 1. WT 6h rep 1 (Cy3), Δ*hrpL* 6h rep 1 (Cy5); 2. Δ*hrpL* 6h rep 2 (Cy3), WT 6h rep 2 (Cy5); 3. WT 6h rep 3 (Cy3), Δ*hrpL* 6h rep 3 (Cy5); 4. Δ*hrpL* 6h rep 4 (Cy3), WT 6h rep 4 (Cy5); 5. Δ*hrpL* 18h rep 1 (Cy3), WT 18h rep 1 (Cy5); 6. WT 18h rep 2 (Cy3), Δ*hrpL* 18h rep 2 (Cy5); 7. Δ*hrpL* 18h rep 3 (Cy3), WT 18h rep 3 (Cy5); 8. WT 18h rep 4 (Cy3), Δ*hrpL* 18h rep 4 (Cy5). This design incorporated a dye-swap and balanced labelling of all samples. Levels and efficiencies of labelling were estimated using a NanoDrop spectrophotometer. Microarray hybridization, washing and scanning were performed in the JHI Sequencing and Microarray Facility as described previously (Stushnoff *et al*., 2010). Microarray images were imported into Agilent Feature Extraction (FE) (v.9.5.3) software and aligned with the appropriate array grid template file (021826_D_F_20081029). Intensity data and quality control (QC) metrics were extracted using the recommended FE protocol (GE2-v5_95_Feb07). Entire FE datasets for each array were loaded into GeneSpring (v.7.3) software for further analysis. The experimental design and all microarray data are available at ArrayExpress (http://www.ebi.ac.uk/arrayexpress/; accessions: Microarray #A-MEXP-2000, Dataset #E-TABM-1137).

Microarray analysis

Data were normalized using default settings for two-channel arrays: data were transformed to account for dye-swaps and data from each array were normalized using the Lowess algorithm to minimize differences in dye incorporation efficiency. Unreliable data flagged as absent in all replicate samples by the FE software were discarded. Significantly changing gene lists were generated from combined replicate datasets for each time point using volcano plot filtering (fold-change ratio >1.5×; Student's *t*-test P value < 0.05). None of these represented potentially ambiguous probes (e.g. pseudogenes or plasmid genes), which would have required a more careful investigation.

Bioinformatics

Nucleic and amino acid sequences were managed using the Lasergene® 7.2.0 software suite (DNASTAR, Madison, WI, USA) and annotated in agreement with the *E. amylovora* ATCC 49946 genome (Sebaihia *et al*., 2010). The similarity of DNA and protein sequences was determined using cognate BLAST programs at NCBI (http://blast.ncbi.nlm.nih.gov/Blast.cgi) (Altschul *et al*., 1997). Genes of interest were analysed for GC content with GC-Profile (http://tubic.tju.edu.cn/GC-Profile) (Gao and Zhang, 2006) and putative transmembrane domains using the DAS transmembrane prediction server http://www.sbc.su.se/~miklos/DAS) (Cserzo *et al*., 1997). Signal peptides were predicted using SignalP 3.0 (http://www.cbs.dtu.dk/services/SignalP/) (Bendtsen *et al*., 2004). All nucleic and amino acid alignments were created using T-Coffee multiple sequence alignment software (http://www.tcoffee.org/homepage.html) (Notredame *et al*., 2000). Weblogo 2.8.2 (http://weblogo.berkeley.edu) was used to visualize multiple sequence alignments (Crooks *et al*., 2004).

Hidden Markov modelling of *hrp* promoter

To identify HrpL *cis*-regulatory elements in the genome of *E. amylovora*, sequence training sets were assembled including 54 *hrp* promoters from *Erwinia*, *Pectobacterium*, *Dickeya* and *Pantoea* species (Holeva *et al*., 2004; Oh and Beer, 2005; Shrestha *et al*., 2008; Wei *et al*., 2000). Promoter sequences were 28 or 29 bp in length and flanked by canonical '–35' and '–10' HrpL-binding sites (Table S1, see Supporting Information). Sequences were aligned with T-coffee multiple alignment software and the resulting alignment was used to construct a hidden Markov model with the hmmbuild and hmmcalibrate functions of HMMer 2.3.2 (Eddy, 1998). Our HrpL promoter model was then tested against the genome of *E.*

amylovora ATCC 49946 (NCBI: NC_013971) (Sebaihia *et al*., 2010) using the HMMer function hmmsearch, with a bit-score classifier threshold of 8.5. Predicted *hrp* promoters were then sorted empirically on the basis of three criteria: (i) location in intergenic space; (ii) orientation relative to annotated genes in *E. amylovora* ATCC 49946; and (iii) E-values less than those of *hrp* promoters with known HrpL-dependent activity. The reported results were experimentally verified using qRT-PCR. The hidden Markov model described above is available on request.

qRT-PCR and cDNA synthesis

To validate the gene expression patterns identified in our microarray experiment and to explore the HrpL regulon as revealed using bioinformatic techniques, qRT-PCR was performed using RNA isolations independent of the samples used for microarray hybridization. RNA was extracted as described above. First-strand cDNA synthesis was conducted with 1 μg of total RNA and Taqman Reverse Transcription Reagents (Applied Biosystems, Foster City, CA, USA) according to the manufacturer's protocol. Residual RNA was degraded with RNase H (Invitrogen, Carlsbad, CA, USA). After determining the primer efficiencies, 20-μL qRT-PCRs were performed using SYBR Green PCR Master Mix (Applied Biosystems). Primers were designed using Primer Express 3.0 (Applied Biosystems) and the sequences are listed in Table S2 (see Supporting Information). All reactions were conducted with a StepOne Plus Real-Time PCR System (Applied Biosystems) and amplification was carried out with one polymerase activation cycle at 95 °C for 10 min, followed by 40 cycles: denaturation at 95 °C for 15 s and annealing at 60 °C for 1 min. Nonspecific primer activity was monitored using a dissociation curve and the resulting threshold cycles (C_T) were determined using StepOne Software 2.1 (Applied Biosystems) software. All reactions were normalized against the endogenous control *gyrA* (Takle *et al*., 2007) and C_T data were analysed quantitatively via the comparative C_T method to generate relative fold-change values comparing WT and Ea1189Δ*hrpL* transcript abundance. Each qRT-PCR analysis was performed in triplicate and repeated three times.

Biofilm formation *in vitro* crystal violet assay

The biofilm formation abilities of Ea1189 strains were explored using a modified crystal violet assay described previously (Koczan *et al*., 2009; O'Toole *et al*., 1999). Ea1189 strains were grown overnight to 2×10^8 cfu/mL. Cultures were diluted to 0.2 OD_{600} in 0.5 × LB broth and a 25-μL suspension was combined with 2 mL of sterile 0.5 × LB broth in a 24-well polystyrene plate (Corning, New York City, NY, USA). To quantify biofilm formation, a glass cover-slip was added to each plate well at a 30° angle to maximize surface contact with the inoculated medium. The plates were then incubated at 28 °C for 48 h. Following incubation, culture suspensions were removed, replaced with 10% crystal violet and allowed to stain at room temperature for 1 h. Crystal violet was then decanted and glass cover-slips and plate wells were washed gently three times with water before air drying overnight. For qualitative analysis, crystal violet pigment accumulation, representing biofilm formation, was observed and recorded from plate well walls and cover-slips. For quantitative analysis, crystal violet was resolubilized from glass coverslips using 200 μL of 40% methanol, 10% glacial acetic acid. A Safire microplate reader (Tecan, Research Triangle Park, NC, USA) was then utilized at an absorbance of 600 nm to quantify solubilized crystal violet via spectrophotometry. The biofilm formation abilities of each Ea1189 strain were assayed three times with 12 replicates per assay.

Motility assay

To assess the swarming motility of Ea1189, WT and mutant strains were cultured overnight to 2×10^8 cfu/mL, collected by centrifugation and washed once with 0.5 × PBS. Each sample was then resuspended to 0.2 OD_{600} in 0.5 × PBS and 10 μL of diluted sample was added to the centre of swarming agar plates (10 g tryptone, 5 g NaCl, 3 g agar per litre of water) as described previously (Hildebrand *et al*., 2006; Skerker *et al*., 2005). Swarming diameters were recorded for each sample after 24 and 48 hpi at 28 °C. The assay was repeated three times with 10 replicates per experiment.

ACKNOWLEDGEMENTS

We thank Janette Jacobs and Lee Duynslager for assistance in the early stages of this work, as well as Maria M. Lopez and Pablo Llop (Departamento de Protección Vegetal y Biotecnología, Instituto Valenciano de Investigaciones Agrarias, Valencia, Spain) for the pEI70 plasmid sequences used for microarray design. This work was supported by a special grant from the United States Department of Agriculture (USDA) CSREES to GWS, the Agricultural Experiment Stations of Michigan and Illinois, Project GREEEN (Generating Research and Extension to Meet Economic and Environmental Needs), a Michigan plant agriculture initiative at Michigan State University, the Agriculture and Food Research Initiative Competitive Grants Program Grant no. 2010–65110-20497 to YFZ from the USDA National Institute of Food and Agriculture, the Scottish Government Rural and Environment Research and Analysis Directive (RERAD) and the UK Biotechnology and Biological Sciences Research Council (BBSRC).

REFERENCES

Aldridge, P., Metzger, M. and Geider, K. (1997) Genetics of sorbitol metabolism in *Erwinia amylovora* and its influence on bacterial virulence. *Mol. Gen. Genet.* **256**, 611–619.

Altschul, S.F., Madden, T.L., Schaffer, A.A., Zhang, J., Zhang, Z., Miller, W. and Lipman, D.J. (1997) Gapped BLAST and PSI-BLAST: a new generation of protein database search programs. *Nucleic Acids Res.* **25**, 3389–3402.

Asselin, J.E., Oh, C.-S., Nissinen, R.M. and Beer, S.V. (2006) The secretion of EopB from *Erwinia amylovora*. *Acta Hortic.* **704**, 409–415.

Barny, M.A., Guinebretiere, M.H., Marcais, B., Coissac, E., Paulin, J.P. and Laurent, J. (1990) Cloning of a large gene cluster involved in *Erwinia amylovora* CFBP1430 virulence. *Mol. Microbiol.* **4**, 777–786.

Barragan, M.J.L., Blazquez, B., Zamarro, M.T., Manchen, J.M., Garcia, J.L., Diaz, E. and Carmona, M. (2005) BzdR, a repressor that controls the anaerobic catabolism of benzoate in *Azoarcus* sp. CIB, is the first member of a new subfamily of transcriptional regulators. *J. Biol. Chem.* **280**, 10 683–10 694.

Bauer, D.W. and Beer, S.V. (1991) Further characterization of an hrp gene cluster *Erwinia amylovora*. *Mol. Plant–Microbe Interact.* **4**, 493–499.

Bendtsen, J.D., Nielsen, H., von Heijne, G. and Brunak, S. (2004) Improved prediction of signal peptides: SignalP 3.0. *J. Mol. Biol.* **340**, 783–795.

Bocsanczy, A.M., Nissinen, R.M., Oh, C.-S. and Beer, S.V. (2008) HrpN of *Erwinia amylovora* functions in the translocation of DspA/E into plant cells. *Mol. Plant Pathol.* **9**, 425–434.

Burse, A., Weingart, H. and Ullrich, M.S. (2004) The phytoalexin-inducible multidrug efflux pump AcrAB contributes to virulence in the fire blight pathogen, *Erwinia amylovora*. *Mol. Plant–Microbe Interact.* **17**, 43–54.

Büttner, D. and He, S.Y. (2009) Type III protein secretion in plant pathogenic bacteria. *Plant Physiol.* **150**, 1656–1664.

Cesbron, S., Paulin, J.-P., Tharaud, M., 1, Barny, M.-A. and Brisset, M.-N. (2006) The alternative σ factor HrpL negatively modulates the flagellar system in the phytopathogenic bacterium *Erwinia amylovora* under *hrp*-inducing conditions. *FEMS Microbiol. Lett.* **257**, 221–227.

Chatterjee, A., Cui, Y., Chaudhuri, S. and Chatterjee, A.K. (2002a) Identification of regulators of hrp/hop genes of *Erwinia carotovora* ssp. *carotovora* and characterization of $HrpL_{Ecc}$ ($SigmaL_{Ecc}$), an alternative sigma factor. *Mol. Plant Pathol.* **3**, 359–370.

Chatterjee, A., Cui, Y. and Chatterjee, A.K. (2002b) Regulation of *Erwinia carotovora* $hrpL_{Ecc}$ (*sigma-*L_{Ecc}), which encodes an extracytoplasmic function subfamily of sigma factor required for expression of the HRP regulon. *Mol. Plant–Microbe Interact.* **15**, 971–980.

Cock, P.J.A., Antao, T., Chang, J.T., Chapman, B.A., Cox, C.J., Dalke, A., Friedberg, I., Hamelryck, T., Kauff, F., Wilczynski, B. and de Hoon, M.J. (2009) Biopython: freely available Python tools for computational molecular biology and bioinformatics. *Bioinformatics*, **25**, 1422–1423.

Crooks, G.E., Hon, G., Chandonia, J.-M. and Brenner, S.E. (2004) WebLogo: a sequence logo Generator. *Genome Res.* **14**, 1188–1190.

Cserzo, M., Wallin, E., Simon, I., von Heijne, G. and Elofsson, A. (1997) Prediction of transmembrane α-helices in prokaryotic membrane proteins: the dense alignment surface method. *Protein Eng.* **10**, 673–676.

Datsenko, K.A. and Wanner, B.L. (2000) One step inactivation of chromosomal genes in *Escherichia coli* K-12 using PCR products. *Proc. Natl. Acad. Sci. USA*, **97**, 6640–6645.

Degrassi, G., Devescovi, G., Bigirimana, J. and Venturi, V. (2010) *Xanthomonas oryzae* pv. *oryzae* XKK.12 contains an AroQγ chorismate mutase that is involved in rice virulence. *Phytopathology*, **100**, 262–270.

Eddy, S.R. (1998) Profile hidden Markov models. *Bioinformatics*, **14**, 755–763.

Faize, M., Brisset, M.N., Perino, C., Vian, B., Barny, M.A., Paulin, J.P. and Tharaud, M. (2006) Protection of apple against fire blight induced by *hrpL* mutant of *Erwinia amylovora*. *Biol. Plant.* **50**, 667–674.

Ferreira, A.O., Myers, C.R., Gordon, J.S., Martin, G.B., Vencato, M., Collmer, A., Wehling, M.D., Alfano, J.R., Moreno-Hagelsieb, G., Warren, F., Lamboy, W.F., DeClerck, G., Schneider, D.J. and Cartinhour, S.W. (2006) Whole-genome expression profiling defines the HrpL regulon of *Pseudomonas syringae* pv. *tomato* DC3000, allows *de novo* reconstruction of the Hrp *cis* element, and identifies novel coregulated genes. *Mol. Plant–Microbe Interact.* **11**, 1167–1179.

Foster, G.C., McGhee, G.C., Jones, A.L. and Sundin, G.W. (2004) Nucleotide sequences, genetic organization, and distribution of pEU30 and pEL60 from *Erwinia amylovora*. *Appl. Environ. Microbiol.* **70**, 7539–7544.

Fouts, D.E., Abramovitch, R.B., Alfano, J.R., Baldo, A.M., Buell, C.R., Cartinhour, S., Chatterjee, A.K., D'Ascenzo, M., Gwinn, M.L., Lazarowitz, S.G., Lin, N.-C., Martin, G.B., Rehm, A.H., Schneider, D.J., van Dijk, K., Tang, X. and Collmer, A. (2002) Genomewide identification of *Pseudomonas syringae* pv. *tomato* DC3000 promoters controlled by the HrpL alternative sigma factor. *Proc. Natl. Acad. Sci. USA*, **99**, 2275–2280.

Gao, F. and Zhang, C.-T. (2006) GC-Profile: a web-based tool for visualizing and analyzing the variation of GC content in genomic sequences. *Nucleic Acids Res.* **34**, 686–691.

Gerstmeir, R., Cramer, A., Dangel, P., Schaffer, S. and Eikmanns, B.J. (2004) RamB, a novel transcriptional regulator of genes involved in acetate metabolism of *Corynebacterium glutamicum*. *J. Bacteriol.* **186**, 2798–2809.

He, S.Y. and Jin, Q. (2003) The Hrp pilus: learning from flagella. *Curr. Opin. Microbiol.* **6**, 15–19.

Hildebrand, M., Aldridge, P. and Geider, K. (2006) Characterization of *hns* genes from *Erwinia amylovora*. *Mol. Genet. Genomics*, **275**, 310–319.

Hogenhout, S.A., Van der Hoorn, R.A.L., Terauchi, R. and Kamoun, S. (2009) Emerging concepts in effector biology of plant-associated organisms. *Mol. Plant–Microbe Interact.* **22**, 115–122.

Holeva, M.C., Bell, K.S., Hyman, L.J., Avrova, A.O., Whisson, S.C., Birch, P.R.J. and Toth, I.K. (2004) Use of a pooled transposon mutation grid to demonstrate roles in disease development for *Erwinia carotovora* subsp. *atroseptica* putative type III secreted effector (DspE/A) and helper (HrpN) proteins. *Mol. Plant–Microbe Interact.* **17**, 943–950.

Hutcheson, S.W., Bretz, J., Sussan, T., Jin, S. and Pak, K. (2001) Enhancer-binding proteins HrpR and HrpS interact to regulate hrp-encoded Type III protein secretion in *Pseudomonas syringae* strains. *J. Bacteriol.* **183**, 5589–5598.

Huynh, T.V., Dahlbeck, D. and Staskawicz, B.J. (1989) Bacterial blight of soybean: regulation of a pathogen gene determining host cultivar specificity. *Science*, **245**, 1374–1377.

Innes, R.W., Bent, A.F., Kunkel, B.N., Bisgrove, S.R. and Staskawicz, B.J. (1993) Molecular analysis of avirulence gene *avrRpt2* and identification of a putative regulatory sequence common to all known *Pseudomonas syringae* avirulence genes. *J. Bacteriol.* **175**, 4859–4869.

Jones, J.T., Furlanetto, C., Bakker, E., Banks, B., Blok, V., Chen, Q., Phillips, M. and Prior, A. (2003) Characterization of a chorismate mutase from the potato cyst nematode *Globodera pallida*. *Mol. Plant Pathol.* **4**, 43–50.

Kiely, P.D., O'Callaghan, J., Abbas, A. and O'Gara, F. (2008) Genetic analysis of genes involved in dipeptide metabolism and cytotoxicity in *Pseudomonas aeruginosa* PAO1. *Microbiology*, **154**, 2209–2218.

Koczan, J.M., McGrath, M.T., Zhao, Y. and Sundin, G.W. (2009) Contribution of *Erwinia amylovora* exopolysaccharides amylovoran and levan to biofilm formation: implications in pathogenicity. *Phytopathology*, **99**, 1237–1244.

Kovach, M.E., Elzer, P.H., Hill, D.S., Robertson, G.T., Farris, M.A., Roop, II, R.M. and Peterson, K.M. (1995) Four new derivatives of the broad-host-range cloning vector pBBR1MCS, carrying different antibiotic-resistance cassettes. *Gene*, **166**, 175–176.

Kube, M., Migdoll, A.M., Müller, I., Kuhl, H., Beck, A., Reinhardt, R. and Geider, K. (2008) The genome of *Erwinia tasmaniensis* strain Et1/99, a non-pathogenic bacterium in the genus *Erwinia*. *Environ. Microbiol.* **10**, 2211–2222.

Lan, L., Deng, X., Zhou, J. and Tang, X. (2006) Genome-wide gene expression analysis of *Pseudomonas syringae* pv. *tomato* DC3000 reveals overlapping and distinct pathways regulated by *hrpL* and *hrpRS*. *Mol. Plant–Microbe Interact.* **9**, 976–987.

McGhee, G.C. and Jones, A.L. (2000) Complete nucleotide sequence of ubiquitous plasmid pEA29 from *Erwinia amylovora* strain Ea88: gene organization and intraspecies variation. *Appl. Environ. Microbiol.* **66**, 4897–4907.

Merighi, M., Majerczak, D.R., Stover, E.H. and Coplin, D.L. (2003) The HrpX/HrpY two-component system activates *hrpS* expression, the first step in the regulatory cascade controlling the Hrp regulon in *Pantoea stewartii* subsp. *stewartii*. *Mol. Plant–Microbe Interact.* **3**, 238–248.

Nissan, G., Manulis, S., Weinthal, D.M., Sessa, G. and Barash, I. (2005) Analysis of promoters recognized by HrpL, an alternative σ-factor protein from *Pantoea agglomerans* pv. *gypsophilae*. *Mol. Plant–Microbe Interact.* **7**, 634–643.

Nissinen, R.M., Ytterberg, A.J., Bogdanove, A.J., van Wijk, K.J. and Beer, S.V. (2007) Analyses of the secretomes of *Erwinia amylovora* and selected *hrp* mutants reveal novel type III secreted proteins and an effect of HrpJ on extracellular harpin levels. *Mol. Plant Pathol.* **8**, 55–67.

Notredame, C., Higgins, D.G. and Heringa, J. (2000) T-Coffee: a novel method for fast and accurate multiple sequence alignment. *J. Mol. Biol.* **302**, 205–217.

Oh, C.S. and Beer, S.V. (2005) Molecular genetics of *Erwinia amylovora* involved in the development of fire blight. *FEMS Microbiol. Lett.* **253**, 85–192.

Oh, C.-S., Kim, J.F. and Beer, S.V. (2005) The *hrp* pathogenicity island of *Erwinia amylovora* and identification of three novel genes required for systemic infection. *Mol. Plant Pathol.* **6**, 125–138.

Ortiz-Martín, I., Thwaites, R., Macho, A.P., Mansfield, J.W. and Beuzon, C.R. (2010) Positive regulation of the Hrp type III secretion system in *Pseudomonas syringae* pv. *phaseolicola*. *Mol. Plant–Microbe Interact.* **5**, 665–681.

O'Toole, G., Pratt, L., Watnick, P., Newman, D., Weaver, V. and Kolter, R. (1999) Genetic approaches to study of biofilms. *Methods Enzymol.* **310**, 91–107.

Sambrook, J.F., Fritsch, E.F. and Maniatis, T.P. (1989) *Molecular Cloning: A Laboratory Manual*, 2nd edn, Vol. **2**. Cold Spring Harbor, NY: Cold Spring Harbor Laboratory Press.

Sanchez-Torres, V., Maeda, T. and Wood, T.K. (2010) Global regulator H-NS and lipoprotein NlpI influence production of extracellular DNA in *Escherichia coli*. *Biochem. Biophys. Res. Commun.* **401**, 197–202.

Sebaihia, M., Bocsanczy, A.M., Biehl, B.S., Quail, M.A., Perna, N.T., Glasner, J.D., DeClerck, G.A., Cartinhour, S., Schneider, D.J., Bentley, S.D., Parkhill, J. and Beer, S.V. (2010) Complete genome sequence of the plant pathogen *Erwinia amylovora* strain ATCC 49946. *J. Bacteriol.* **192**, 2020–2021.

Shen, H. and Keen, N.T. (1993) Characterization of the promoter of avirulence gene D from *Pseudomonas syringae* pv. *tomato*. *J. Bacteriol.* **175**, 5916–5924.

Shrestha, R., Park, D.H., Cho, J.M., Cho, S., Wilson, C., Hwang, I., Hur, J.H. and Lim, C.K. (2008) Genetic organization of the *hrp* genes cluster in *Erwinia pyrifoliae* and characterization of HR active domains in $HrpN_{Ep}$ protein by mutational analysis. *Mol. Cells*, **25**, 30–42.

Skerker, J.M., Prasol, M.S., Perchuk, B.S., Biondi, E.G. and Laub, M.T. (2005) Two-component signal transduction pathways regulating growth and cell cycle progression in a bacterium: a system-level analysis. *PLoS Biol.* **3**, e334.

Smits, T.H.M., Rezzonico, F., Kamber, T., Blom, J., Goesmann, A., Frey, J.E. and Duffy, B. (2010) Complete genome sequence of the fire blight pathogen *Erwinia amylovora* CFBP 1430 and comparison with the other *Erwinia* spp. *Mol. Plant–Microbe Interact.* **23**, 384–393.

Sreedharan, A., Penaloza-Vazquez, A., Kunkel, B.N. and Bender, C.L. (2006) CorR regulates multiple components of virulence in *Pseudomonas syringae* pv. *tomato* DC3000. *Mol. Plant–Microbe Interact.* **19**, 768–779.

Stushnoff, C., Ducreux, L.J.M., Hancock, R.D., Hedley, P.E., Holm, D., McDougall, G.J., McNicol, J.W., Morris, J., Morris, W.L., Sungurtas, J., Verall, S., Zuber, T. and Taylor, M. (2010) Flavonoid profiling and transcriptome analysis reveals new gene–metabolite correlations in tubers of *Solanum tuberosum* L. *J. Exp. Bot.* **61**, 1225–1238.

Takle, G.W., Toth, I.K. and Brurberg, M.B. (2007) Evaluation of reference genes for real-time RT-PCR expression studies in the plant pathogen *Pectobacterium atrosepticum*. *BMC Plant Biol.* **7**, 50.

Teng, C.H., Tseng, Y.T., Maruvada, R., Pearce, D., Xie, Y., Paul-Satyaseela, M. and Kim, K.S. (2010) NlpI contributes to *Escherichia coli* K1 strain RS218 interaction with human brain microvascular endothelial cells. *Infect. Immun.* **78**, 3090–3096.

Triplett, L.R., Melotto, M. and Sundin, G.W. (2009) Functional analysis of the N terminus of the *Erwinia amylovora* secreted effector DspA/E reveals features required for secretion, translocation, and binding to the chaperone DspB/F. *Mol. Plant–Microbe Interact.* **22**, 1282–1292.

Tyson, J.W., Chapman, J., Hugenholtz, P., Allen, E.E., Ram, R.J., Richardson, P.M., Solovyev, V.V., Rubin, E.M., Rokhsar, D.S. and Banfield, J.F. (2004) Community structure and metabolism through reconstruction of microbial genomes from the environment. *Nature*, **428**, 37–43.

Vencato, M., Tian, F., Alfano, J.R., Buell, C.R., Cartinhour, S., DeClerck, G.A., Guttman, D.S., Stavrinides, J., Joardar, V., Lindeberg, M., Bronstein, P.A., Mansfield, J.W., Myers, C.R., Collmer, A. and Schneider, D.J. (2006) Bioinformatics-enabled identification of the HrpL regulon and type III secretion system effector proteins of *Pseudomonas syringae* pv. *phaseolicola* 1448A. *Mol. Plant–Microbe Interact.* **19**, 1193–1206.

Venkatesh, B., Babujee, L., Liu, H., Hedley, P., Fujikawa, T., Birch, P., Toth, I. and Tsuyumu, S. (2006) *Erwinia chrysanthemi* 3937 PhoQ sensor kinase regulates several virulence determinants. *J. Bacteriol.* **188**, 3088–3098.

Wang, L. and Beer, S.V. (2006) Application of signature-tagged mutagenesis to the study of virulence of *Erwinia amylovora*. *FEMS Microbiol. Lett.* **265**, 164–171.

Wei, Z.M. and Beer, S.V. (1995) hrpL activates *Erwinia amylovora* hrp gene transcription and is a member of the ECF subfamily of sigma factors. *J. Bacteriol.* **177**, 6201–6210.

Wei, Z.M., Sneath, B.J. and Beer, S.V. (1992) Expression of *Erwinia amylovora* hrp genes in response to environmental stimuli. *J. Bacteriol.* **174**, 1875–1882.

Wei, Z., Kim, J.F. and Beer, S.V. (2000) Regulation of *hrp* genes and type III protein secretion in *Erwinia amylovora* by HrpX/HrpY, a novel two-component system, and HrpS. *Mol. Plant–Microbe Interact.* **13**, 1251–1262.

Wilson, C.G., Kajander, T. and Regan, L. (2005) The crystal structure of NlpI: a prokaryotic tetratricopeptide repeat protein with a globular fold. *FEBS J.* **272**, 166–179.

Xiao, Y. and Hutcheson, S.W. (1994) A single promoter sequence recognized by a newly identified alternate sigma factor directs expression of pathogenicity and host range determinants in *Pseudomonas syringae*. *J. Bacteriol.* **176**, 3089–3091.

Xiao, Y., Heu, S., Yi, J., Lu, Y. and Hutcheson, S.W. (1994) Identification of a putative alternate sigma factor and characterization of a multicomponent regulatory cascade controlling the expression of *Pseudomonas syringae* pv. *syringae* Pss6l *hrp* and *hrmA* genes. *J. Bacteriol.* **176**, 1025–1036.

Yang, S., Perna, N.T., Cooksey, D.A., Okinaka, Y., Lindow, S.E., Ibekwe, M., Keen, N.T. and Yang, C.-H. (2004) Genome-wide identification of plant-upregulated genes of *Erwinia chrysanthemi* 3937 using a GFP-based IVET leaf array. *Mol. Plant–Microbe Interact.* **17**, 999–1008.

Yang, S., Peng, Q., Zhang, Q., Zou, L., Li, Y., Robert, C., Pritchard, L., Liu, H., Hovey, R., Wang, Q., Birch, P., Toth, I.K. and Yang, C.-H. (2010) Genome-wide identification of HrpL-regulated genes in the necrotrophic phytopathogen *Dickeya dadantii* 3937. *PLoS ONE*, **5**, e13472.

Yap, M.-N., Yang, C.-H., Barak, J.D., Jahn, C.E. and Charkowski, A.O. (2005) The *Erwinia chrysanthemi* type III secretion system is required for multicellular behavior. *J. Bacteriol.* **187**, 639–648.

Zhao, Y., Blumer, S.E. and Sundin, G.W. (2005) Identification of *Erwinia amylovora* genes induced during infection of immature pear tissue. *J. Bacteriol.* **187**, 8088–8103.

Zhao, Y., He, S.Y. and Sundin, G.W. (2006) The *Erwinia amylovora avrRpt2*$_{Ea}$ gene contributes to virulence on pear and AvrRpt2$_{Ea}$ is recognized by *Arabidopsis* RPS2 when expressed in *Pseudomonas syringae*. *Mol. Plant–Microbe Interact.* **19**, 644–654.

Zhao, Y., Sundin, G.W. and Wang, D. (2009a) Construction and analysis of pathogenicity island deletion mutants of *Erwinia amylovora*. *Can. J. Microbiol.* **55**, 457–464.

Zhao, Y.F., Wang, D., Nakka, S., Sundin, G.W. and Korban, S.S. (2009b) Systems level analysis of two-component signal transduction systems in *Erwinia amylovora*: role in virulence, regulation of amylovoran biosynthesis and swarming motility. *BMC Genomics*, **10**, 245.

Zwiesler-Vollick, J., Plovanich-Jones, A.E., Nomura, K., Bandyopadhyay, S., Joardar, V., Kunkel, B.N. and He, S.Y. (2002) Identification of novel *hrp*-regulated genes through functional genomic analysis of the *Pseudomonas syringae* pv. *tomato* DC3000 genome. *Mol. Microbiol.* **45**, 1207–1218.

SUPPORTING INFORMATION

Additional Supporting Information may be found in the online version of this article:

Table S1 Sequences used to construct hidden Markov *hrp* promoter models.

Table S2 Quantitative real-time PCR primers used in this study.

Please note: Wiley-Blackwell are not responsible for the content or functionality of any supporting materials supplied by the authors. Any queries (other than missing material) should be directed to the corresponding author for the article.

